

# Vibration performance characteristics of a long-span and light-weight concrete floor under human-induced loads

Liang Cao<sup>1,2a</sup>, Jiepeng Liu<sup>\*1,2</sup>, Xuhong Zhou<sup>1,2b</sup> and Y. Frank Chen<sup>3b</sup>

<sup>1</sup>School of Civil Engineering, Chongqing University, Chongqing, China

<sup>2</sup>Key Laboratory of New Technology for Construction of Cities in Mountain Area (Chongqing University), Ministry of Education, Chongqing, 400045, China

<sup>3</sup>Department of Civil Engineering, The Pennsylvania State University, Middletown, USA

(Received May 12, 2016, Revised December 8, 2017, Accepted December 23, 2017)

**Abstract.** An extensive research was undertaken to study the vibration serviceability of a long-span and light-weight floor subjected to human loading experimentally and numerically. Specifically, heel-drop test was first conducted to capture the floor's natural frequencies and damping ratios, followed by jumping and running tests to obtain the acceleration responses. In addition, numerical simulations considering walking excitation were performed to further evaluate the vibration performance of a multi-panel floor under different loading cases and walking rates. The floor is found to have a high frequency (11.67 Hz) and a low damping ratio (2.32%). The comparison of the test results with the published data from the 1997 AISC Design Guide 11 indicates that the floor exhibits satisfactory vibration perceptibility overall. The study results show that the peak acceleration is affected by the walking path, walking rate, and adjacent structure. A simpler loading case may be considered in design in place of a more complex one.

**Keywords:** vibration serviceability; concrete floor; human-induced loads; loading case; peak acceleration

## 1. Introduction

The floor is an integral part of a building (industrial, commercial, residential, or public). Building occupants anticipate that the vibration of the building floor will remain at an acceptable level under normal conditions. When the floor slab vibrates excessively, the occupants may feel annoyed or alarmed. The cost to solve a potential floor vibration problem would be high. Floor vibration has emerged as the second most frequent source of complaints from building users (Chen *et al.* 2016).

The design of a long-span and light-weight floor for a modern public structure such as that of Beijing Yintai Center (Lv *et al.* 2007) is often governed by serviceability rather than strength requirements (Rijal *et al.* 2015, Van Nimmen *et al.* 2017, Zivanovic *et al.* 2005). The performance of the floor under human activities such as walking, running, and aerobics dancing should be checked against certain vibration acceptability criterion. A vibration exceeding a certain serviceability limit may arise, disturbing occupants or an equipment. To avoid a possible serious and costly vibration problem caused by the human activities (Dorvash *et al.* 2014), an extensive study is therefore carried out to examine the dynamic characteristics of the floor.

For more than a decade, the issue of human-induced vibration has been investigated on various floor systems by researchers using field measurement (An *et al.* 2016, Nakamura and Kawasaki 2006, Pavic *et al.* 2008, Zhou *et al.* 2016a, c), finite element (FE) method (Abeyasinghe *et al.* 2013, Brownjohn *et al.* 2016, Chen 1999, Petrovic-Kotur and Pavic 2016, Zivanovic and Pavic 2009), and theoretical analysis (Chen *et al.* 2014a, Zhou *et al.* 2016a, b). As a result, various vibration acceptability criteria have been proposed and included in the design codes including AS 2670.2 (1990), 1997 AISC Design Guide 11 (Murray *et al.* 1997), AS 2670.1 (2001), ISO 10137 (2007), GB 50010-2010 (2010), and JGJ 3-2010 (2010). In reviewing the literature, it appears that the vibration assessment criteria are primarily related to modal properties (fundamental natural frequency, damping ratio) and acceleration thresholds.

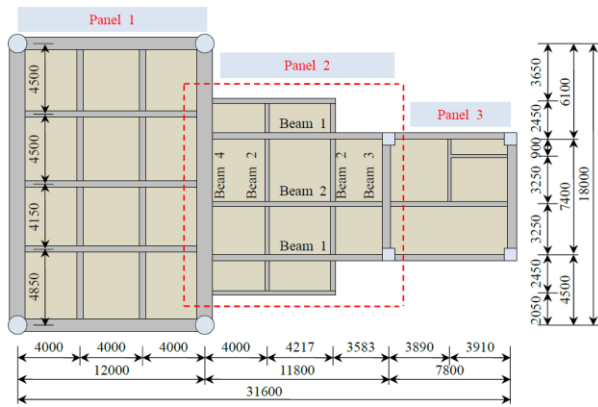
This paper discusses the vibration performance of a long-span and light-weight concrete floor slab, intended to be used in an airport lounge in Chongqing City, China based on the field test and finite element analysis results. Specifically, heel-drop test was first conducted to capture the floor's natural frequencies and damping ratios, followed by jumping and running tests to obtain the acceleration responses. The airport lounge is a multi-panel floor structure, which is somewhat inactive to human activities. However, the effect of the response from the adjacent active panels on the less active floor has not been fully studied (Sandun De Silva and Thambiratnam 2009). Hence, it is warranted to evaluate the responses of both active and inactive panels and their effects, considering different possible load paths. Through the numerical simulations, the

\*Corresponding author, Professor

E-mail: [liujp@cqu.edu.cn](mailto:liujp@cqu.edu.cn)

<sup>a</sup>Ph.D.

<sup>b</sup>Professor



(a) Overall structural layout of the floor (mm)

No. of Beam	$b$	$h$
Beam 1	400	800
Beam 2	300	750
Beam 3	500	800
Beam 4	1000	1200

(b) the detailed beam cross sections (mm)

Fig. 1 The investigated floor system

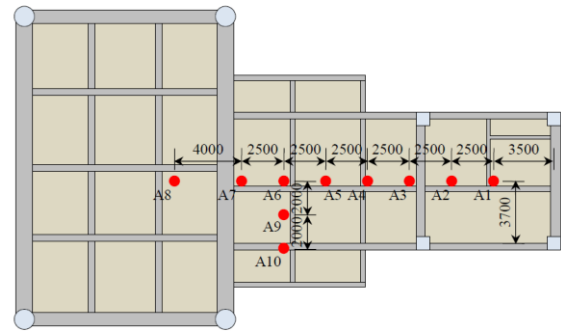
dynamic characteristics of the multi-panel concrete floor subjected to walking vibrations with different walking rates were determined.

## 2. Description of prototype floor, tests, and numerical simulation

Field testing and numerical simulation are necessary to determine the dynamic properties of the floor subjected to human-induced dynamic loads and further to evaluate the floor's vibration performance (Chen *et al.* 2014b, Kaito *et al.* 2005). In this study heel-drop impact tests were conducted to capture the dynamic behaviour of the structure and impulsive jumping load and rhythm excitations (running, walking) were considered to evaluate the dynamic floor responses.

The investigated structure is a floor consisting of 150 mm thick concrete slab as shown in Fig. 1(a) with detailed supporting-beam cross sections indicated in Fig. 1(b). The elastic modulus  $E$  of the concrete is  $3.25 \times 10^4$  MPa. The footprint for Panel 2 considered in the experiment is shown in dashed lines in Fig. 1(a). The floor was completed prior to the installation of any nonstructural component (e.g., ceiling, vent pipe, mechanical equipment, and partition), i.e., the floor is in the pre-fitout stage.

The measurement system consists of ten accelerometers with the acceleration capability of  $\pm 5g$  ( $g$  = the gravitational acceleration) and a data acquisition system. Fig. 2(a) shows the schematic locations of these accelerometers (i.e., measuring points) used subsequently to facilitate the characterization of the measurements during a test process. To better understand the effects of various system parameters, field tests considering heel-drop, jumping, and



(a) Measuring points (mm)



(b) Accelerometer DH610V



(c) Signal acquisition

Fig. 2 Measuring points and data acquisition system

running loads were conducted. The data acquisition system was used to sample all the results collected from the accelerometers at a frequency as high as 1000 Hz.

Through the finite element (FE) analyses, the natural frequencies of the floor system were obtained. The FE method was subsequently used to evaluate the dynamic characteristics of the multi-panel concrete floor under walking excitation.

## 3. Modal parameters analysis

Modal properties including natural frequencies, damping ratios, and mode shapes are the important parameters for evaluating floor vibration serviceability. There are several methods available to identify these dynamic parameters. One common method is the heel-drop test as it is easier to be performed and requires no expensive equipment (Blakeborough and Williams 2003). Hence, heel-drop impact tests were first carried out in this study to ascertain those important system parameters. These impact tests initiated at locations A4, A5, and A6 (Fig. 2(a)).

### 3.1 Natural frequencies and modal shape

The acceleration signals and responses measured at

Table 1 Coefficients  $\alpha_1$  and  $\alpha_2$  and theoretical fundamental natural frequencies  $f_1$  under different boundary conditions

Boundary condition	Coefficients		Frequency (Hz)
	$\alpha_1$	$\alpha_2$	
SSFF	13.98	0.5	7.25
SCFF	$\pi^2$	2.56	11.58
CCFF	8.05	8	16.70

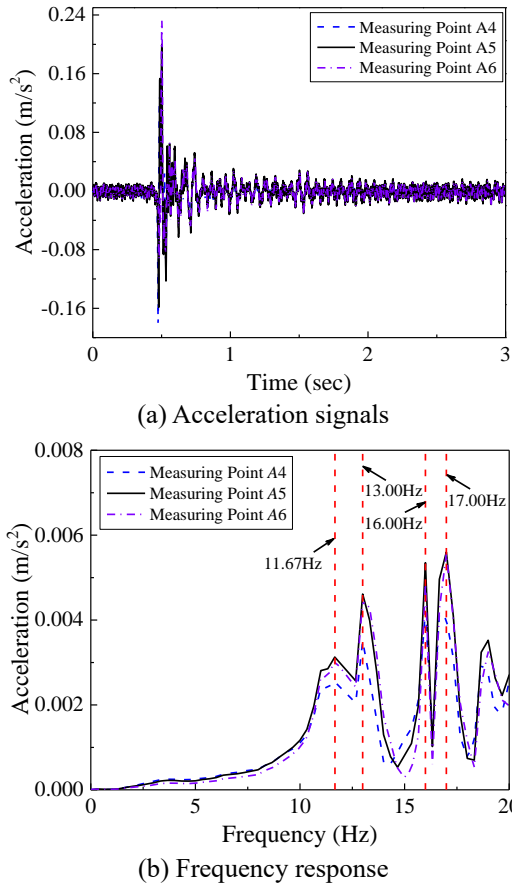
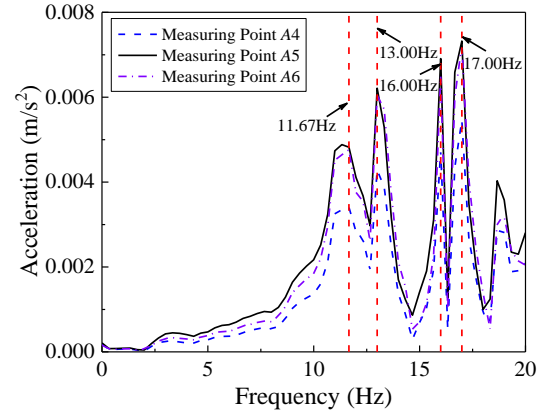


Fig. 3 Results corresponding to the excitation at point A4

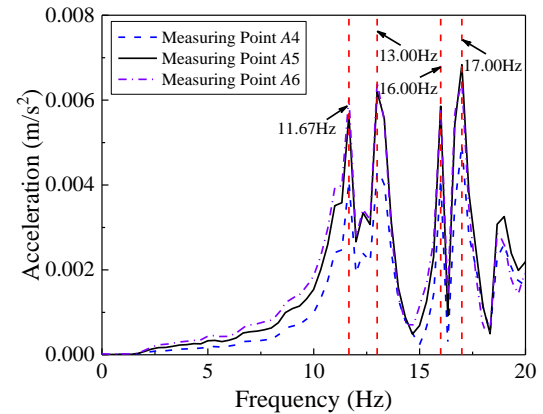
points A4, A5, and A6 corresponding to the excitation at point A4 are shown in Fig. 3. The acceleration signals were transformed to the frequency responses (Fig. 3(b)) by the fast Fourier transform. Likewise, the frequency responses corresponding to excitation points A5 and A6 are shown in Fig. 4. The responses indicate the first three natural frequencies of the floor are 11.67 Hz, 13.00 Hz, and 16.00 Hz, respectively. The floor is relatively rigid compared to the recommended frequency of 10 Hz for practical use by Smith *et al.* (2009).

Similar to the work done by Cao (1983) and Zhou *et al.* (2016a, b), the floor can be idealized as an anisotropic rectangular thin plate. The following simplified/practical formula for determining the fundamental natural frequency of vertical vibration is recommended in this study

$$f_1 = \frac{1}{2\pi} \frac{\alpha_1}{b^2} \sqrt{\frac{g}{q_0}} \sqrt{\frac{\alpha_2 D_1}{C^4}} \quad (1)$$



(a) Excitation at point A5



(b) Excitation at point A6

Fig. 4 The frequency responses

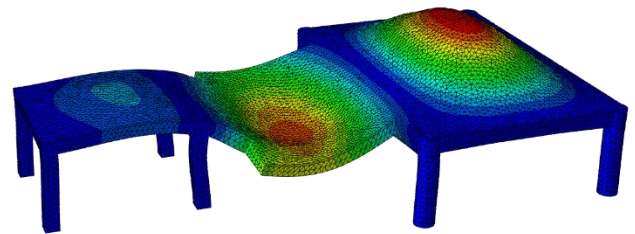


Fig. 5 3D model for the floor using ABAQUS (C3D10 elements)

where  $C = a/b$  being the ratio of beam span  $a$  to plate width  $b$ ;  $D_1$  is the flexible stiffness of the plate ( $= 2.24 \times 10^8 \text{ N}\cdot\text{m}$ );  $\alpha_1$  and  $\alpha_2$  are the coefficients depending on the boundary condition (see Table 1);  $g$  is the gravity acceleration; and  $q_0$  is the load per unit area of the plate ( $= 5331.2 \text{ N/m}^2$ ).

In this paper, three kinds of the boundary conditions were considered: SSFF—simply supported on two opposite edges and free on the other two edges; SCFF—simply supported on one edge, clamped on the opposite edge, and free on the other two edges; and CCFF—clamped on two opposite edges and free on the other two edges. The theoretical fundamental natural frequency  $f_1$  under each boundary condition is indicated in Table 1. The differences between the analytical and the experimental results are 37.87%, 0.77%, and 43.10% for the three boundary conditions, respectively. So, the boundary condition SCFF is deemed more reasonable for a theoretical analysis.

Table 2 The first damping ratio  $\zeta_1$  of the floor (%)

Test #	Measuring point			Average
	A4	A5	A6	
1	2.27	2.38	2.17	2.27
2	2.41	2.52	2.27	2.40
3	1.97	2.04	2.87	2.29

For complex structures, the dynamic performance can be evaluated using the finite element (FE) method. Fig. 5 shows the three-dimensional (3D) FE model and the fundamental mode shape ( $f_1 = 11.08$  Hz), in which C3D10 elements (10-node general quadratic tetrahedron elements) available in ABAQUS program were used. The fundamental natural frequency obtained by the FE analysis differs from the experimental value by 5.05%.

### 3.2 Damping ratios

Damping is another important design consideration. It generally implies the dissipation of energy. Namely, it reduces the floor vibration and eventually diminishes the oscillation. Based on the collected acceleration signal data obtained from the heel-drop tests, the damping ratio  $\zeta$  for lightly damped systems can be determined from (Chopra 1995)

$$\zeta = \frac{1}{2\pi j} \ln \frac{a_i}{a_{i+j}} \quad (2)$$

where  $a_i$  and  $a_{i+j}$  are the  $i$ th and  $i+j$ th measured peak accelerations, respectively.

The heel-drop tests were performed three times at location A5 (Fig. 2). According to the 1997 AISC Design Guide 11 (Murray *et al.* 1997), all vibration modes except one must be filtered from the record of vibration decays to determine the damping. In this paper, a band-pass filter capable of passing a certain range of frequencies is adopted to handle the filtering issue. Table 2 lists the individual and average values of first damping ratios  $\zeta_1$  for the three selective locations. Since  $\zeta_1$  values do not vary significantly among the three tests, an overall average  $\zeta_1$  value of 2.32% (i.e., average of 2.27%, 2.40%, and 2.29%) may be used. Note that  $\zeta_1$  for a floor without non-structural elements as the case in this study is lower than that with non-structural elements. So, the modal damping ratios presented in this paper are conservative in terms of acceleration responses.

## 4. Vibration responses under human-induced loads: Field tests

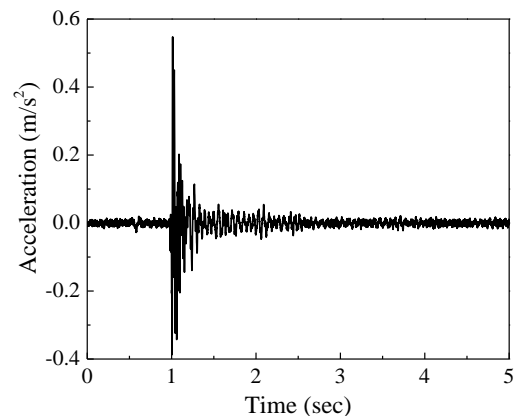
To evaluate the vibration performance of the floor due to human activities, a series of field tests were conducted, including impulsive jumping load and running excitation.

### 4.1 Impulse excitation

To determine the vibration performance of the floor due to the impulse excitation, jumping tests were conducted, as



(a) Volunteer jumping on the floor



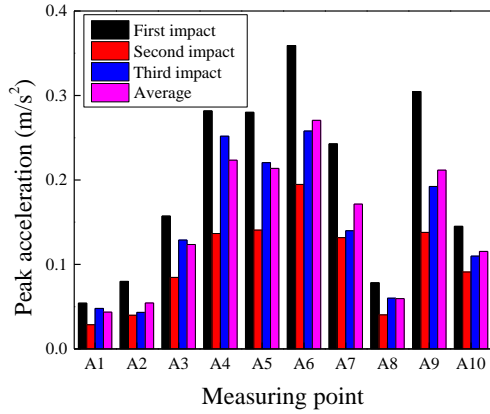
(b) Typical acceleration response

Fig. 6 The jumping test

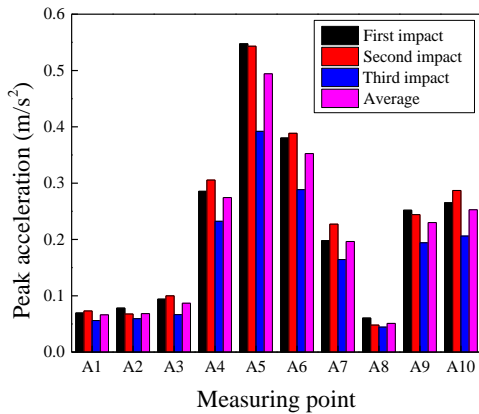
shown in Fig. 6(a). The jumping action was selected as the representative impulse excitation in this study as it is generally regarded as the most severe human loading (Racic and Pavic 2010). The jumping tests initiated at locations A4, A5, A6, and A7 (Fig. 2). To reduce the randomness, the jumping tests were performed three times at each excitation point. Fig. 6(b) shows the typical acceleration response. The peak accelerations at the various measuring points from the jumping tests are shown in Fig. 7. The maximum average acceleration occurred when the excitation was imposed at point A5 ( $\approx 5000$ mm right from the center of Panel 2, Figs. 2 & 1) and the value is  $0.49 \text{ m/s}^2 (= 5\%g)$ .

### 4.2 Rhythm excitation

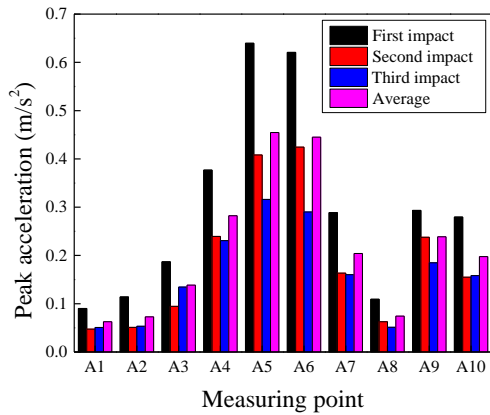
Human response to floor motion is a very complex phenomenon, involving the magnitude of the motion, the surrounding environment, and the human perception. A rhythm excitation could be more annoying than the infrequent or transient motion. So, running tests were performed to estimate the floor's vertical acceleration response, by two representative persons weighted at 63 kg ( $N_{m1}$ ), and 70 kg ( $N_{m2}$ ), respectively. The actual frequencies of running in the daily life were adopted. To obtain the pace frequency, the progress of experimental tests is recorded using a video device, Vidicon. Based on the video data recorded from  $N_{m1}$  and  $N_{m2}$ , the pace frequency is found to be 2.68 Hz and 2.71 Hz, respectively.



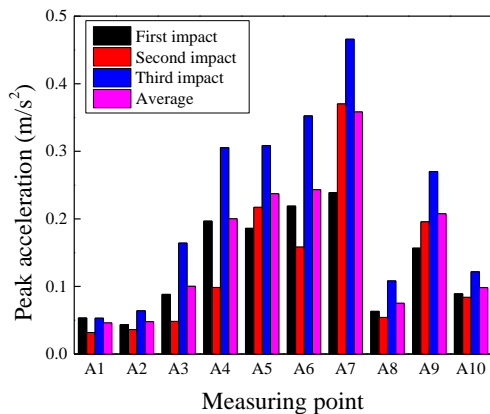
(a) Excitation point A4



(b) Excitation point A5



(c) Excitation point A6



(d) Excitation point A7

Fig. 7 Peak accelerations at various measuring points

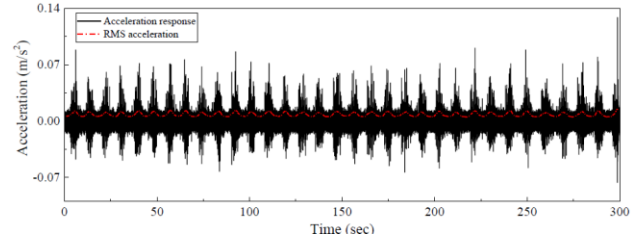
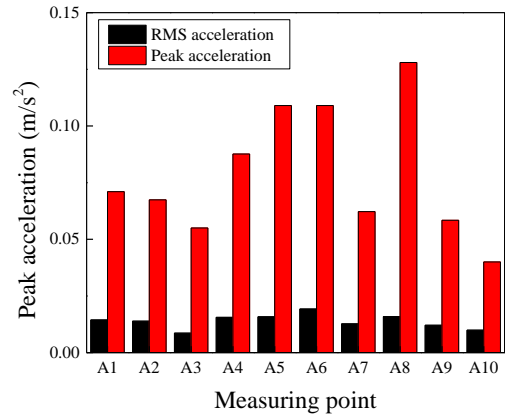
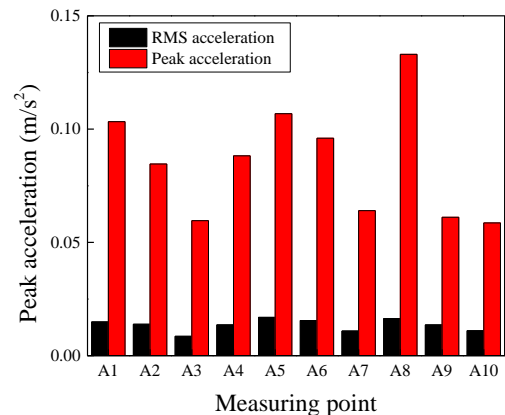


Fig. 8 Typical acceleration responses and RMS accelerations



(a)  $N_{m1}$



(b)  $N_{m2}$

Fig. 9 The peak acceleration and RMS acceleration at each measuring point

Starting from location A4 (Fig. 2), each volunteer ran along the following route repeatedly for a duration of 5 minutes: A4→A8→A1→A8→A1 (Fig. 2). Fig. 8 shows the typical acceleration responses measured from the running tests and the RMS accelerations.

The acceleration responses of the floor were evaluated in terms of root-mean square (RMS) accelerations (Eq. (3)) as they give a better indication on vibration variations (Smith *et al.* 2009)

$$a_{rms}(t) = \sqrt{\frac{1}{N} \sum_{i=1}^N a_i^2(t)} \quad (3)$$

where  $a_{rms}(t)$  is the rolling RMS acceleration at time  $t$ ,  $N$  is the number of acceleration data points from  $t-1$  to  $t+1$ , and  $a_i(t)$  is the  $i$ th acceleration data point.



Table 6 Ratios of the maximum peak acceleration under LC2 to that under LC3

Ratio	Measuring points						
	A11	A12	A13	A14	A15	A16	A17
$\beta$	1.01	1.10	1.03	0.98	1.00	0.98	0.98

### 5.3 Dynamic analysis

A comprehensive dynamic analysis for the floor under the loads described above was carried out. For each loading case, three different walking rates of 1.8, 2.0, and 2.2 Hz were considered to obtain the acceleration responses at locations A11-A17 with A12, A14, and A16 at the centers of Panel 1, Panel 2, and Panel 3, respectively (Fig. 10).

The peak accelerations for loading case LC1 under the three different walking rates are presented in Fig. 11. The figure shows that the peak accelerations at measuring points A11-A17 are inversely proportional to the walking rate  $f$ . For example, the peak accelerations at A11 for walking Route 1 under the three ascending walking rates are 0.073 m/s<sup>2</sup>, 0.060 m/s<sup>2</sup>, and 0.054 m/s<sup>2</sup>, respectively. The peak accelerations are greater for the walking routes perpendicular to the girder than those parallel to the girder. For example, the peak acceleration at A11 under the walking rate 1.8 Hz is 0.073 m/s<sup>2</sup> for Route 1, while it is 0.021 m/s<sup>2</sup> for Route 2 (Figs. 10 & 11). In terms of the effect from the adjacent structure, the trend is reversed. For instance, the ratio of A14 to A13 responses under walking rate 1.8 Hz is 0.89 for Route 2, while it is 0.23 for Route 1.

The peak accelerations of loading cases LC2 and LC3 under walking rate 1.8 Hz are shown in Fig. 12. Table 6 lists the ratios of the maximum peak acceleration under LC2 ( $A_{LC2}$ ) to that under LC3 ( $A_{LC3}$ ), i.e.  $\beta = A_{LC2}/A_{LC3}$ . The  $\beta$  ratios indicate that the simpler load combination (i.e., LC2) may be considered in design instead of the more complex one.

## 6. Vibration responses under human-induced loads: Numerical simulation

Table 7 summarizes the damping ratios and maximum accelerations obtained from the tests (field and numerical simulation) and the vibration limits from the 1997 AISC Guide 11 (Murray *et al.* 1997), where the RMS acceleration for running and walking and the peak acceleration for jumping are assumed. Note that the RMS acceleration induced by walking excitation is calculated by the following formula (Zhou *et al.* 2016a)

$$a_{rms} = 0.2a_{peak} \tag{6}$$

As indicated in Table 7, the damping ratios and accelerations induced by the human activities (excepting jumping) generally satisfy the vibration criteria of the 1997 AISC Design Guide 11 (Murray *et al.* 1997).

## 7. Conclusions

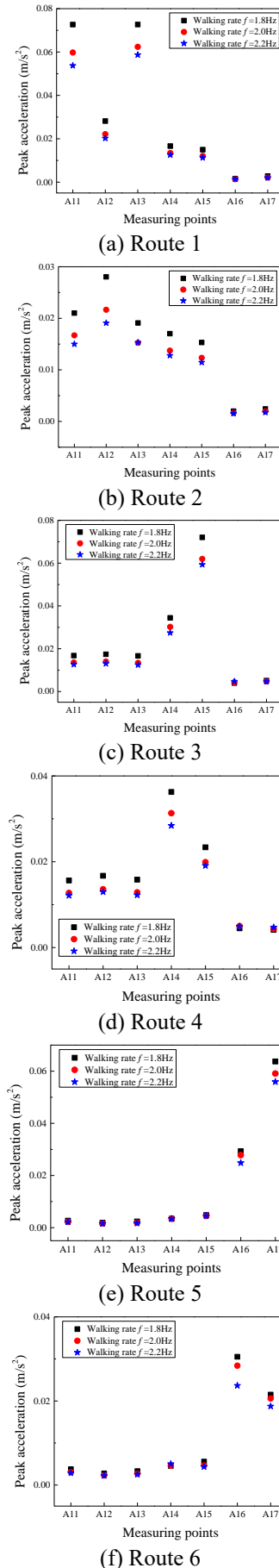


Fig. 11 The RMS acceleration of loading case LC1

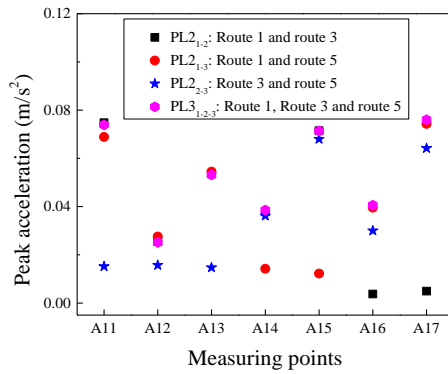


Fig. 12 The peak accelerations for loading cases LC2 and LC3 under walking rate 1.8 Hz

Table 7 Comparison of vibration performance and criteria limits

	Human activity	Test result	Criteria limit
Damping ratio (%)	Heel-drop	2.32	2.00
	Jumping	5.00	
Acceleration (%g)	Walking	0.15	1.50
	Running	0.17	

An extensive research was undertaken to investigate the vibration performance characteristics of a long-span and light-weight concrete floor subjected to human activities experimentally and numerically. Field tests considering heel-drop, jumping impact, and running excitations and numerical simulations for walking excitation were carried out to ascertain the dynamic properties of the concrete floor system. Based on the study results, the following key findings are observed:

- The fundamental natural frequency  $f_1$  of the floor is 11.67 Hz which is higher than the normally recommended practical value of 10 Hz. This indicates that the investigated floor is relatively rigid.
- The analytical floor  $f_1$  values obtained from the simplified/practical formula, Eq. (1), differ from the experimental results respectively by 37.87%, 0.77%, and 43.10% for SSFF, SCFF, and CCFF boundary conditions. The boundary condition SCFF is therefore recommended.
- The ratio of the RMS acceleration to the peak accelerations induced from the running is approximately equal to 0.17.
- The experimental and numerical results indicate that the floor system generally satisfies the vibration criteria of the 1997 AISC Guide 11.
- The numerical results show that the peak accelerations induced by the walking excitation are inversely proportional to the walking rate  $f$  and that the peak accelerations are greater for the walking routes perpendicular to the supporting girders than those parallel to the girders.
- Conversely, the effect from the adjacent structure is greater for the walking routes parallel to the girders than those perpendicular to the girders. A simpler load combination (e.g., LC2, Table 4 & Fig. 10) may be considered in design in lieu of a more complex one (e.g., LC3).

## Acknowledgments

The authors wish to express their gratitude to National Natural Science Foundation of China (51622802) and Chongqing Basic and Frontier Research Project (cstc2014jcyjys30001) for supporting this study.

## References

- Abeysinghe, C.M., Thambiratnam, D.P. and Perera, N.J. (2013), "Dynamic performance characteristics of an innovative hybrid composite floor plate system under human-induced loads", *Compos. Struct.*, **96**, 590-600.
- An, Q., Ren, Q.Y., Liu, H.B., Yan, X.Y. and Chen, Z.H. (2016), "Dynamic performance characteristics of an innovative cable supported beam structure-concrete slab composite floor system under human-induced loads", *Eng. Struct.*, **117**, 40-57.
- AS 2670.1 (2001), *Mechanical Vibration and Shock Human Effects. Evaluation of Human Exposure to Whole-Body Vibration Part 1: General Requirements*, Australia Committee AV-010, Australia.
- AS 2670.2 (1990), *Mechanical Vibration and Shock Human Effects. Evaluation of Human Exposure to Whole-Body Vibration Part 2: Continuous and Shock-Induced Vibration in Buildings (1 to 80 Hz)*, Australia Committee AV-010, Australia.
- Bachmann, H. (1995), *Vibration Problems in Structures*, Birkhauser Verlag AG, Boston.
- Blakeborough, A. and Williams, M.S. (2003), "Measurement of floor vibrations using a heel drop test", *Proceedings of the Institution of Civil Engineers: Structures and Buildings*, **156**(4), 367-371.
- Brownjohn, J., Racic, V. and Chen, J. (2016), "Universal response spectrum procedure for predicting walking-induced floor vibration", *Mech. Syst. Sign. Pr.*, **70-71**, 741-755.
- Cao, G.X. *Vibration of Elastic Rectangular Thin Plate*, China Architecture & Building Press, China.
- Chen, J., Xu, R.T. and Zhang, M.S. (2014a), "Acceleration response spectrum for predicting floor vibration due to occupant walking", *J. Sound Vibr.*, **333**(15), 3564-3579.
- Chen, J., Yan, S.X. and Zhang, M.S. (2014b), "Vibration performance assessment of a long-span concrete floor using field measurement over a five-year period", *Adv. Struct. Eng.*, **17**(8), 1145-1158.
- Chen, J., Zhang, M.S. and Liu, W. (2016), "Vibration serviceability performance of an externally prestressed concrete floor during daily use and under controlled human activities", *J. Perform. Constr. Fac.*, **30**(2), 04015007.
- Chen, Y.C. (1999), "Finite element analysis for walking vibration problems for composite precast building floors using ADINA: Modeling, simulation, and comparison", *Comput. Struct.*, **72**(1), 109-126.
- Chopra, A.K. (1995), *Dynamics of Structures Theory and Application to Earthquake Engineering*, 2nd Edition, Prentice Hall, U.S.A.
- Dorvash, S., Pakzad, S., Naito, C., Hodgson, I. and Yen, B. (2014), "Application of state-of-the-art in measurement and data analysis techniques for vibration evaluation of a tall building", *Struct. Infrastruct. E.*, **10**(5), 654-669.
- GB/T4883-2008 (2008), *Statistical Interpretation of Data-Detection and Treatment of Outliers in Normal Sample*, The National Standard of the People's Republic of China, Beijing, China.
- GB50010-2010 (2010), *Code for Design of Concrete Structures*, Ministry of Housing and Urban-Rural Development of the People's Republic of China, Beijing, China.

- ISO 10137 (2007), *Bases for Design of Structures-Serviceability of Buildings and Walkways against Vibrations*, International Organization for Standardization.
- JGJ 3-2010 (2010), *Technical Specification for Concrete Structures of Tall Buildings*, Ministry of Housing and Urban-Rural Development of the People's Republic of China, Beijing, China.
- Kaito, K., Abe, M. and Fujino, Y. (2005), "Development of non-contact scanning vibration measurement system for real-scale structures", *Struct. Infrastruct. E.*, **1**(3), 189-205.
- Lou, Y., Huang, J. and Lv, Z.C. (2012), *Design of Floor System for the Vibration Serviceability*, Science Press, Beijing, China.
- Lv, Z.C., Han, H.J., Huang, J., Li, P.B., Zhao, G.P. and Lou, Y. (2007), "Vibration design of floor systems of Beijing Yintai center", *Build. Struct.*, **37**(11), 20-22.
- Murray, T.M., Allen, D.E. and Ungar, E.E. (1997), *Steel Design Guide Series No. 11: Floor Vibrations due to Human Activity*, American Institute of Steel Construction, Inc. Chicago, U.S.A.
- Nakamura, S.I. and Kawasaki, T. (2006), "Lateral vibration of footbridges by synchronous walking", *J. Constr. Steel Res.*, **62**(11), 1148-1160.
- Pavic, A., Miskovic, Z. and Zivanovic, S. (2008), "Modal properties of beam-and-block pre-cast floors", *IES J. Part A: Civil Struct. Eng.*, **1**(3), 171-185.
- Petrovic-Kotur, S.P. and Pavic, A.P. (2016), "Vibration analysis and FE model updating of lightweight steel floors in full-scale prefabricated building", *Struct. Eng. Mech.*, **58**(2), 277-300.
- Racic, V. and Pavic, A. (2010), "Mathematical model to generate near-periodic human jumping force signals", *Mech. Syst. Sign. Pr.*, **24**(1), 138-152.
- Rijal, R., Samali, B., Shrestha, R. and Crews, K. (2015), "Experiment and analytical study on dynamic performance of timber-concrete beams", *Constr. Build. Mater.*, **75**, 46-53.
- Sandun De Silva, S. and Thambiratnam, D.P. (2009), "Dynamic characteristics of steel-deck composite floors under human-induced loads", *Comput. Struct.*, **87**, 1067-1076.
- Smith, A.L., Hicks, S.J. and Devine, P.J. (2009), *Design of Floors for Vibration: A New Approach*, The Steel Construction Institute, U.K.
- Van Nimmen, K., Van Den Broeck, P., Verbeke, P., Schauvliege, C., Mallie, M., Ney, L. and De Roeck, G. (2017), "Numerical and experimental analysis of the vibration serviceability of the Bears' Cage footbridge", *Struct. Infrastruct. E.*, **13**(3), 390-400.
- Zhou, X.H., Cao, L., Chen, Y.F., Liu, J.P. and Li, J. (2016a), "Experimental and analytical studies on the vibration serviceability of pre-stressed cable RC truss floor systems", *J. Sound Vibr.*, **361**, 130-147.
- Zhou, X.H., Cao, L., Chen, Y.F., Liu, J.P. and Li, J. (2016b), "Acceleration response of prestressed cable RC truss floor system subjected to heel-drop loading", *J. Perform. Constr. Fac.*, **30**(5), 04016014.
- Zhou, X.H., Li, J. and Liu, J.P. (2016c), "Vibration of pre-stressed cable RC truss floor system due to human activities", *J. Struct. Eng.-ASCE*, **142**(5), 04015170.
- Zivanovic, S. and Pavic, A. (2009), "Probabilistic modeling of walking excitation for building floors", *J. Perform. Constr. Fac.*, **23**(3), 132-143.
- Zivanovic, S., Pavic, A. and Reynolds, P. (2005) "Vibration serviceability of footbridges under human-induced excitation: A literature review", *J. Sound Vibr.*, **279**(1-2), 1-74.